

Purdue University
Purdue e-Pubs

International Compressor Engineering Conference

School of Mechanical Engineering

1990

The Noise Source Identification of Refrigeration Compressor by Signal Processing Technique

J. E. Oh

Han Yang University

H. Park

Han Yang University

C. H. Lee

Goldstar Co.

Follow this and additional works at: <https://docs.lib.purdue.edu/icec>

Oh, J. E.; Park, H.; and Lee, C. H., "The Noise Source Identification of Refrigeration Compressor by Signal Processing Technique" (1990). *International Compressor Engineering Conference*. Paper 752.
<https://docs.lib.purdue.edu/icec/752>

This document has been made available through Purdue e-Pubs, a service of the Purdue University Libraries. Please contact epubs@purdue.edu for additional information.

Complete proceedings may be acquired in print and on CD-ROM directly from the Ray W. Herrick Laboratories at <https://engineering.purdue.edu/Herrick/Events/orderlit.html>

THE NOISE SOURCE IDENTIFICATION OF REFRIGERATION COMPRESSOR BY SIGNAL PROCESSING TECHNIQUE

* J. E. OH

** H. PARK

*** C. H. LEE

* Associate Professor
Department of Precision Mechanical Engineering
Hanyang Univ., Seoul, Korea

** Graduate Student
Department of Precision Mechanical Engineering
Hanyang Univ., Seoul, Korea

*** Researcher
Home Appliance Research Laboratory
Lucky - Goldstar Co., Seoul, Korea

ABSTRACT

It is well known that the major noise source of a refrigerator is the compressor, and due to the tendency of higher quality and more lighter weight of manufactured goods, the importance of prevention and reduction of noise is increasing.

In this paper, in order to prevent and reduce such noise, sound pressure level and acoustic intensity are measured for the compressor, and the results of these measurements, the noise radiation characteristics of the compressor are identified. Also the experimental modal analysis is applied to the compressor to identify the noise source.

INTRODUCTION

Recently, noise and vibration problems are on the rise many times in the electrical home appliances, and especially stressed by the trend of lighter weight and higher quality goods. It is complicated to find the generating source and propagating path of noise in the compressor which are the main noise source in a refrigerator. The rotating forces generated from the driving unit in the compressor act as compression force and rise to mechanical vibration and pressure pulsation. Also the forces excite the compressor shell, and produce structure-borne sound and air-borne sound through the propagating path. As the above, noise problem in the electrical home appliances is important factor which determines not only the performance and quality of goods, but also the domestic environment.

For the purpose of producing the noiseless refrigerator that will increase our selling competitive power, it is essential to examine the noise and vibration phenomena and identify the exact generating source to work out a countermeasure by using the various analysis method. In this paper, the noise source identification by measuring sound pressure and acoustic intensity is introduced. And the relation between noise and vibration is also identified by applying modal analysis technique to the compressor.

THEORETICAL ANALYSIS

Basic theory of acoustic intensity

In elasto-acoustic system, the acoustic intensity is a vector quantity defined as a product of the acoustic pressure and the corresponding particle velocity at a given point. When there is no flowing, the one dimensional equation of motion is

$$\rho \frac{\partial u(t)}{\partial t} + \frac{\partial p(t)}{\partial r} = 0 \quad (1)$$

where ρ is the density of air, $u(t)$ is the particle velocity in r -direction. If the acoustic pressure are $p_1(t)$ and $p_2(t)$ measured at two closely-spaced points in r -direction, then the gradient of acoustic pressure is approximately represented as

$$\frac{\partial p(t)}{\partial r} = \frac{p_2(t) - p_1(t)}{\Delta r} \quad (2)$$

where Δr is the distance between two points where the acoustic pressure were measured. Then the approximately particle velocity is

$$\begin{aligned} u(t) &= -\frac{1}{\rho} \int_{-\infty}^{\infty} \frac{\partial p(t)}{\partial r} dt \\ &= -\frac{1}{\rho \Delta r} \int_{-\infty}^{\infty} \{p_2(t) - p_1(t)\} dt \end{aligned} \quad (3)$$

and the acoustic pressure P at the center of two points can be approximated as $p(t) = \{p_1(t) + p_2(t)\}/2$. Therefore the acoustic intensity, I becomes

$$\begin{aligned} I &= \lim_{T \rightarrow \infty} \frac{1}{T} \int_{-\infty}^{\infty} u(t) \cdot p(t) dt = \langle p(t) \cdot u(t) \rangle \\ &= -\frac{1}{\rho \Delta r} \langle \frac{p_1(t) + p_2(t)}{2} \int_{-\infty}^{\infty} \{p_2(t) - p_1(t)\} dt \rangle \end{aligned} \quad (4)$$

where $\langle \rangle$ denotes a time average. By the stationary and ergodic process of signals $\langle p_1(t) \int_{-\infty}^{\infty} p_2(t) dt \rangle$ becomes zero, and using the relation of $\langle p_1(t) \int_{-\infty}^{\infty} p_2(t) dt \rangle = \langle -p_2(t) \int_{-\infty}^{\infty} p_1(t) dt \rangle$, the acoustic intensity of equation (4) can be rewritten as

$$I = -\frac{1}{\rho \Delta r} \langle p_1(t) \int_{-\infty}^{\infty} p_2(\tau) d\tau \rangle \quad (5)$$

By computing Fourier transforms of equation (5), acoustic intensity $I(f_1-f_2)$ in frequency domain is expressed as

$$I(f_1-f_2) = \frac{1}{2\pi\rho\Delta r} \int_{f_1}^{f_2} \frac{\text{Im}\{G_{12}(f)\}}{f} df \quad (6)$$

where Im is the imaginary part of a complex number and $G_{12}(f)$ is cross spectral density function of the acoustic pressures at the two points. Hence acoustic intensity can be determined by measuring the imaginary part of cross-spectrum between the pressure P_1 and P_2 measured at closely-spaced points. In this paper, the 2-channel FFT analyzer was used to compute the acoustic intensity in frequency domain.

Theoretical basis of modal analysis

If the mechanical structure has a damping proportional to the velocity, the dynamic equation will be considered in the matrix form

$$[M]\{\ddot{x}(t)\} + [C]\{\dot{x}(t)\} + [K]\{x(t)\} = \{f(t)\} \quad (7)$$

The damping matrix $[C]$ of eq.(7) is represented by linear sum of mass and stiffness matrix. At this point, if the vibration of each point is represented by linear combination of the vibrational mode, eq.(7) will be as follows:

$$\begin{aligned} \{X\} &= \sum_{r=1}^n \frac{\{\phi_r\}^T \{F\} \{\phi_r\}}{-\omega^2 m_r + j\omega c_r + k_r} \\ &= \sum_{r=1}^n \frac{\{\phi_r\}^T \{F\} \{\phi_r\}}{k_r \left[1 - \left(\frac{\omega}{\omega_n}\right)^2 + j 2 \zeta_r \left(\frac{\omega}{\omega_n}\right) \right]} \\ &= \sum_{r=1}^n \frac{\{\phi_r\}^T \{F\} \{\phi_r\}}{m_r (-\omega^2 + \omega_n^2 + j 2 \zeta_r \omega \omega_n)} \end{aligned} \quad (8)$$

From eq.(8), we know that the transfer function is represented by superposition of each one-degree of freedom system. In practice, it can be measured in a specific range of frequency because of the function of analyzer. The ij component of matrix in the transfer function, that is, the relation between the force at j point and the response of i point is

$$H_{ij} = \frac{X_i}{F_j} = \sum_{r=1}^n \frac{\Phi_{ir} \Phi_{jr}}{\omega^2 m_r + j \omega c_r + k_r} \\ = \sum_{r=1}^n \frac{\Phi_{ir} \Phi_{jr}}{m_r} \cdot \frac{1}{-\omega^2 + \omega_r^2 + j 2 \zeta_r \omega \omega_r} \quad (9)$$

Here, we know the important thing that the denominator of eq.(9) only depends upon natural frequency and damping ratio regardless of exciting point i and measuring point j . The measured transfer functions are some where they are taken at any point of system. From eq.(9), the vibrational mode existing lower and higher effect on the transfer function of measuring range. In practice, if we decide the measuring frequency range, $l-m$, eq.(9) will be transformed as follows:

$$\frac{X_i}{F_j} = \sum_{r=1}^{l-1} \frac{\Phi_{ir} \Phi_{jr}}{\omega^2 m_r} \cdot \frac{1}{\left| 1 - \left(\frac{\omega}{\omega_r} \right)^2 + j 2 \zeta_r \left(\frac{\omega}{\omega_r} \right) \right|} + \sum_{r=l}^m \frac{\Phi_{ir} \Phi_{jr}}{\omega^2 m_r + j \omega c_r + k_r} \\ + \sum_{r=m+1}^n \frac{\Phi_{ir} \Phi_{jr}}{k_r} \cdot \frac{1}{\left| 1 - \left(\frac{\omega}{\omega_r} \right)^2 + j 2 \zeta_r \left(\frac{\omega}{\omega_r} \right) \right|} \quad (10)$$

At lower frequency range than the measuring frequency range, term will be zero; will be zero vice versa. And eq.(10) can be written approximately.

$$\frac{X_i}{F_j} = \sum_{r=1}^{l-1} \frac{\Phi_{ir} \Phi_{jr}}{\omega^2 m_r} + \sum_{r=l}^m \frac{\Phi_{ir} \Phi_{jr}}{\omega^2 m_r + j \omega c_r + k_r} + \sum_{r=m+1}^n \frac{\Phi_{ir} \Phi_{jr}}{k_r} \quad (11)$$

The first and third term of eq.(11) are called inertia restraint and residual flexibility term.

Modal parameters for the transfer function will be obtained by selecting the adequate curve - fitting method depending on characteristics of transfer function.

EXPERIMENTAL APPARATUS AND DATA PROCESSING

The measurement of sound pressure and acoustic intensity

A reciprocating, closed-type compressor is used, which is separated to the faces of front(FR), right(RI), rear(RE), left(LE), and up(UP), in order to examine the noise emitting characteristics of each face. It is measured and analyzed each side of the compressor by dividing 25(5x5) points except the upper side, dividing 36(6x6) points. The measurement of sound pressure and acoustic intensity is carried out under the steady state (suction pressure : 0.1 kgf/cm², discharge pressure : 9.5 kgf/cm²) after operating the compressor. The schematic diagram of measuring and data processing system for sound pressure and acoustic intensity is shown in Fig.1.

All measurements are performed with two 1/2" condenser microphones and a 12 mm spacer. The two microphones are mounted by face to face and the phase error between the microphones is calibrated by a piston phone. The FFT analyzer(SD-375) and the micro computer(IBM-AT) are interfaced by the GPIB interface bus line. The results are represented by the contour and three dimensional plot to identify the accurate noise source of the compressor visually.

Application of experimental modal analysis technique

Each signal measured by the force transducer and accelerometer was converted from analog to digital by the FFT analyzer, and was transmitted to the micro computer. The impact experiment of the compressor shell was carried out for the upper part of it, and for the shell assembly to identify the coupling coefficient.

Also, to find out the influence of the shell components due to the operation of the compressor, it was measured in actual state when it was in and not in operation. Fig.2 shows the measuring points of the internal components suspended by three springs. The mode shape of the structure was determined using the imaginary part of the transfer function obtained by the impact experiment.

EXPERIMENTAL RESULT AND CONSIDERATION

Radiation characteristics by sound pressure and acoustic intensity

Radiation characteristics of each side of the compressor

The experimental result of sound pressure under the steady state after operating the compressor, are shown in Table 1, which was measured by overall level in the anechoic chamber. The coherent rank of the sound pressure of each side, own the response characteristics in order of the right, left, rear, front and upper side.

In order to find the response characteristics of sound pressure at each side, center frequency level is shown in Fig.3 using 1/3 octave band graph. From this figure, the dominant center frequency in the range of measuring frequency is 500Hz and 2kHz. From Table 2, in the case of 500Hz, the coherent order of each side is rear, front, left, right, upper side and in the case of 2kHz, left, front, rear, right, upper side. Contour and three dimensional plot of sound pressure and sound intensity at 500Hz is shown representing in Fig.4 to identify more detail. With comparing of the inner schematic diagram and contour plot at the left side of the suction pipe, the highest level is appeared at the right, lower side of suction pipe connection part. Next, the contour plot of the right side and the left side at 2kHz is shown in Fig.5 and Fig.6 respectively. In the case side, the highest sound pressure is radiated along with suction pipe connection part and silencer at suction part. In the case of right side, it appears the highest level at discharging pipe connection part and left, upper side.

Coherence estimation of noise in each component

The estimation result of sound pressure with coupling the each component of compressor are shown in Table 3. In experiment 1, in case of rotating crank shaft only, the center frequency 6.3Hz represent the highest level of 48.7 dB(A), and it is suppose that it's due to the effect of vibration and friction of crank shaft. While, in case of experiment 2 (exp.1 + cylinder block connected), the center frequency of 500Hz and 2kHz become high, but order frequencies become low, which have no effect on overall level. Experiment 4, valve stopper and muffler dB(A) comparing with exp.3 and they are the major noise source of inside of the compressor. In case of experiment 5, we put valve into between cylinder block and valve stopper, all sound pressure levels become low except 6.3kHz and goes down 3 dB(A) in overall level. Experiment 6, loop pipe is connected with between exhausting side cylinder and exhausting pipe, the noise of high frequency band widths like 4kHz and 6.3kHz are decreased effectively. In case of experiment 7 is the result of joining the upper shell with compressor. In this case, almost frequency band width except 63 Hz shows well-damped effect, and 9.4 dB(A) noise reduction effect at overall level. From the previous results, we come to know that the valve stopper and suctional muffler are the major noise sources in the compressor and loop pipe have good noise reduction effects on high frequency band like 4 kHz and 6.3kHz.

Identification of vibration characteristics by modal analysis

Frequency response characteristics

Fig.7 shows the frequency response characteristics of compressor vibration about the left side, which is the principle noise source. In this figure, each of the peak value is 60Hz, 115Hz, and 175Hz, consisting of harmonic order. Between 480Hz and 650Hz and near 2kHz, it shows relatively high peak value because of the contribution of shell vibration to noise, comparing with the result of sound pressure. The contour plot about 60Hz which denotes the highest vibration level is shown in Fig.8. From this figure, it is found that the highest level of shell vibration is generated from the valve part of front side. While near 500Hz, the highest vibration level is generated from the left central part of the upper side. And near the frequency of 2kHz, in the case of front side, the highest vibration level is generated from left part, and in the case of upper side, from left central part and the reciprocating part of the piston.

Vibration characteristics of shell and mounting

From the experimental results of the vibration characteristics about the various shell model, the upper and lower part of the shell have different vibrational modes respectively, and the vibrational modes between 0Hz and 1800Hz are not appeared and the complex vibrational modes in high frequency range(1800 ~ 5000Hz) are produced according to their welding joint, as shown in Table 4. Also the vibrational modes are shifted comparing with the result of before and after the attachment of mounting to the shell.

While the frequency band which vibrational modes can contribute as noise source in compressor is 4 kHz. At this frequency, the highest sound is generated from upper side as appeared in Fig.9, which is measuring results of sound pressure and also this frequency is the vibrational modes which has the highest level at the upper part of shell. Fig.10 is the measuring results of transfer function for the mounting and shell. Vicinity of 500Hz which was not appeared in shell vibration, is the modes of high level of mounting vibration and this frequency contributes to sound pressure of 500Hz.

Application to inner structure

For the inner structure, it is excited at point 7 shown in Fig.2 and Fig.11 shows transfer function which is calculated by acceleration response at the point 1,2,3 supported by spring. From this figure, it is found that the dominant frequency components are 475Hz and 1275Hz among the complex vibrational mode. And also when point 7 is excited, the transfer function calculated from the response of measuring point 1 (dashed line) which is inside of compressor and the response of measuring point 4 (solid line) which is outside of compressor is shown in Fig.12. From this figure, it can be known that vibration at frequency component of 475Hz is remarkably transferred to the shell, but that of 1275Hz is isolated by the spring and the natural characteristics of the shell. So it is found that the vibrational modes generated from the inner structure contributes to noise of 500Hz which has high sound radiation pressure in the compressor.

CONCLUSION

From the considerations of the experimental results, following conclusions were obtained.

- (1) The dominant frequency bands in 1/3 octave band are 500 Hz and 2 kHz.
- (2) The main source of noise at 500 Hz is the shell vibration, which is generated from the inner part of the compressor due to the motor driving. And this vibration produce the structure-bone sound, leading to the solid body motion of the shell influenced by mounting.
- (3) Noise at 2 kHz has the highest level on the connection part of the suction pipe, which caused by the welding defect and the pipe configuration.
- (4) The highest level of 4 kHz noise is influenced by the vibrational mode of 4 kHz on the upper shell.

Results obtained in this study will be useful data for the design of noise reduced compressor for a refrigerator.

REFERENCES

- 1) S.M. Price and R.J.Bernhard, "Application of Modal Technique to Noise Control of Hermetic Refrigeration Compressors", pp.515-519,1986
- 2) S.H.Kim, "A Study of Noise Source Identification on Plate Excited Structure Borne Sound by Acoustic Intensity Method", M.S.dissertation of Hanyang Univ.,1986
- 3) D.D.Reynolds, " Engineering Principle of Acoustics, Noise and Vibration Control ",Allyn and Bacon,Inc,1981
- 4) D.J.Ewins, " Modal Testing : Theory and Practice ",RSP LTD.,1984
- 5) J.S. Bendat and A.G. Piersol, " Engineering Application of Correlation and Spectral Analysis",Willy Interscience Pub.,1980
- 6) L.L.Faulkner, " Hermetic Refrigeration Compressor Acoustics ",Proceeding of the Purdue Noise Control conference,pp.107-114,1971
- 7) Harold W.Lord, "Noise Control for Engineers", McGraw-Hill,Inc.,1980
- 8) J.D.Irwin and E.R.Graf, "Industrial Noise and Vibration Control ", PRENTICE-HALL,Inc.,1979

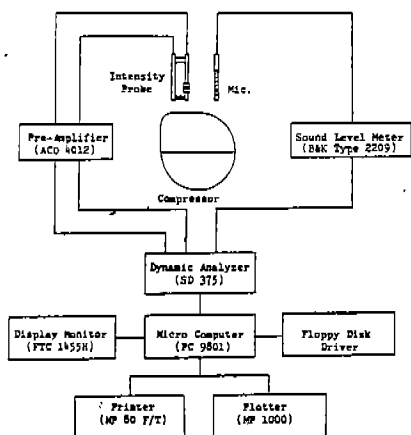


Fig.1 Block diagram of the technique to measure the sound and acoustic intensity

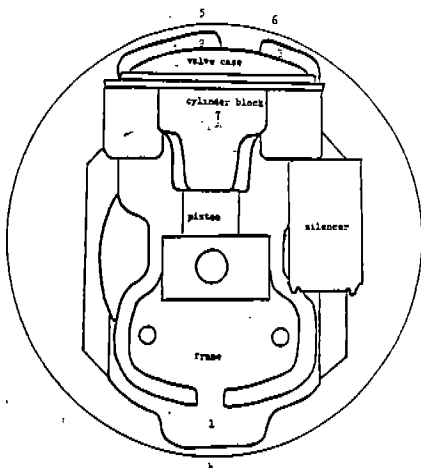


Fig.2 Measuring point of mechanism

Table 1 Contribution of each side by sound pressure level for compressor

Side	Sound pressure level (dBA)				
	FR	RI	RE	LE	UP
Level	38.7	39.5	39.6	40.0	35.5

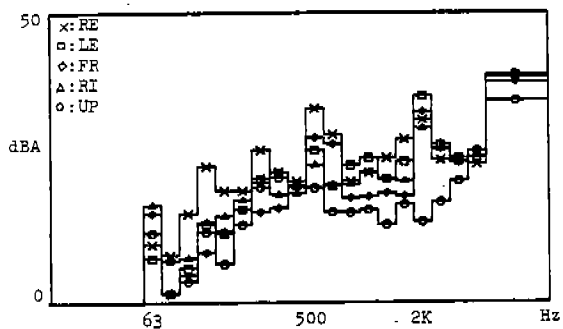


Fig.3 1/3 octave band response of each side for compressor

Table 2 Sound pressure response of each frequency for compressor

Freq.	Sound pressure level (dBA)				
	FR	RT	RE	LE	UP
53	15.7	17.2	10.3	7.9	12.3
80	1.8	7.4	8.4	1.6	1.6
100	5.1	7.9	15.7	6.3	4.0
125	9.0	14.2	24.1	13.9	12.6
160	12.7	15.3	19.7	12.3	7.0
200	16.6	18.3	19.7	16.6	13.9
250	16.1	21.3	26.8	22.0	20.5
315	16.9	19.1	23.0	23.0	22.2
400	20.6	19.4	21.4	20.7	20.6
500	29.2	24.4	33.9	26.9	20.4
630	28.1	20.9	29.4	20.7	16.1
800	18.7	21.1	21.4	24.4	16.0
1k	19.0	23.3	22.9	25.7	16.5
1.25k	19.7	21.9	25.5	22.1	13.9
1.6k	19.1	21.6	28.7	25.1	17.5
2k	33.6	30.7	32.1	36.3	14.4
2.5k	27.3	27.0	25.2	27.9	17.9
3.15k	24.9	25.0	25.0	25.6	21.7
4k	25.9	26.7	24.5	25.7	26.9

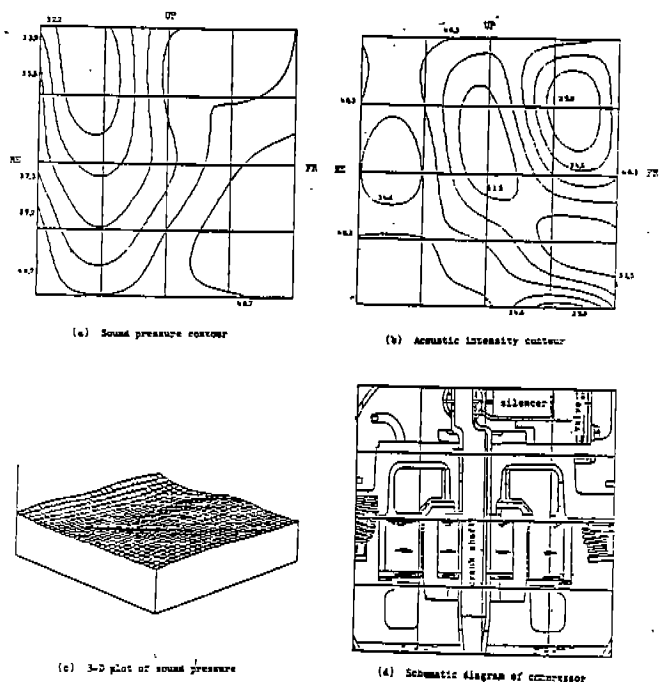


Fig.4 Noise radiation pattern of left side at 500Hz

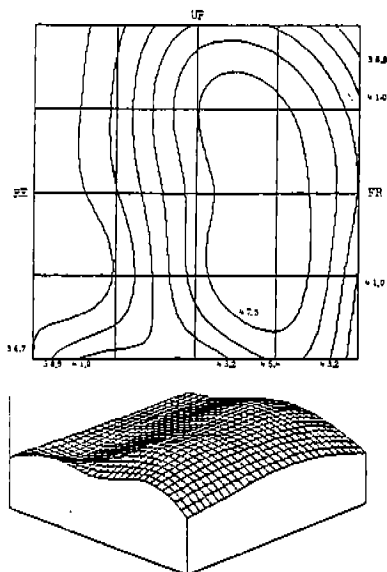


Fig.5 Sound pressure plot of left side at 2kHz

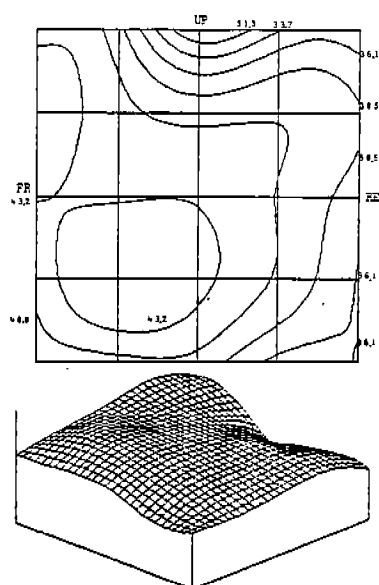


Fig.6 Sound pressure plot of right side at 2kHz

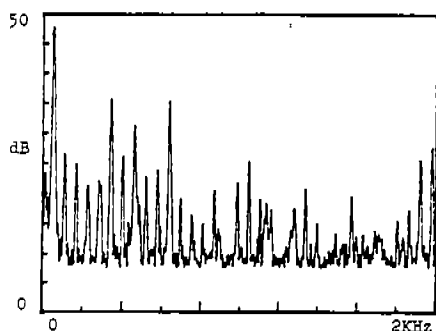


Fig.7 Vibration response characteristics of left side

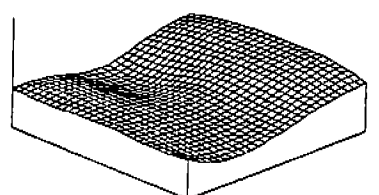
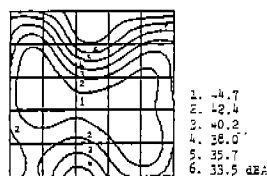


Fig.8 Vibration level plot over front side of compressor at 60Hz

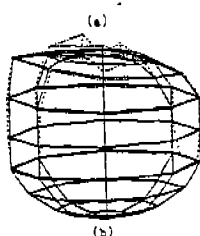


Fig.9 (a) Sound pressure contour of upper side at 4kHz

(b) The 5th mode (4kHz) shape of running compressor shell

Table 3 Contribution of compressor element to noise (dB(A))

Freq. No.	63	500	2 k	4 k	6.3 k	O.A.
1	41.6	28.1	31.4	33.6	48.7	50.0
2	39.8	29.9	35.7	30.5	45.3	50.2
3	43.4	38.7	42.0	40.8	39.1	52.0
4	47.3	62.4	70.7	63.6	67.8	78.9
5	44.9	45.4	57.6	61.9	69.2	76.0
6	49.1	51.9	57.3	53.5	49.4	67.5
7	52.3	27.4	41.1	44.9	40.3	58.1

O.A. : overall

Table 4 Natural frequency of compressor shell and mounting

Mode	upper shell	lower shell (attached mounting)	combined hol- low shell	combined hol- low shell(at- tached mount- ing)	stationary comp.shell	running comp.shell	mounting (attached shell)
1	337.5	337.5	1862.5	1900.0	2175.0	2662.5	325.0
2	887.5	612.5	2350.0	2312.5	2562.5	2962.5	1212.5
3	1612.5	925.0	2775.0	2812.5	2687.5	3362.5	1650.0
4	2525.0	1612.5	3037.5	3062.5	3012.5	3712.5	2025.0
5	3587.5	2550.0	3437.5	3462.5	3325.0	4600.0	2125.0
6	3750.0	2812.5	3650.0	3625.0	4775.0		3050.0
7	3950.0	3487.5	3750.0	3750.0			3375.0
8	4400.0	3675.0	3850.0	3850.0			4225.0
9			4037.5	4037.5			
10			4750.0	4775.0			

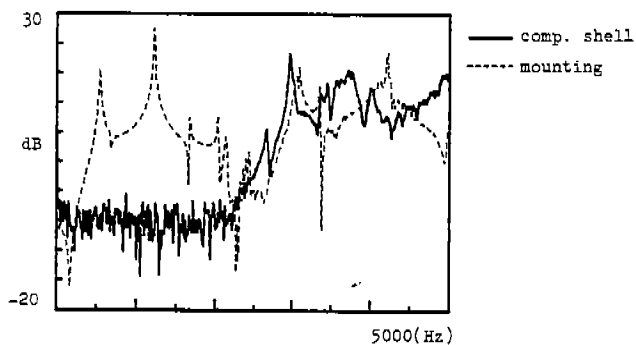


Fig.10 Transfer function for compressor shell and mounting

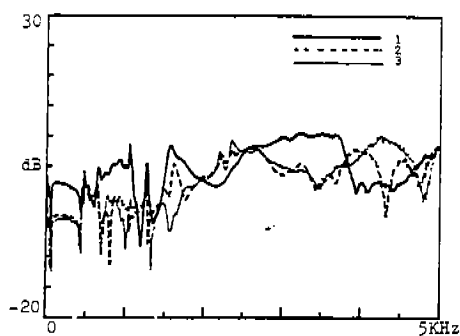


Fig.11 Transfer function of compressor mechanism

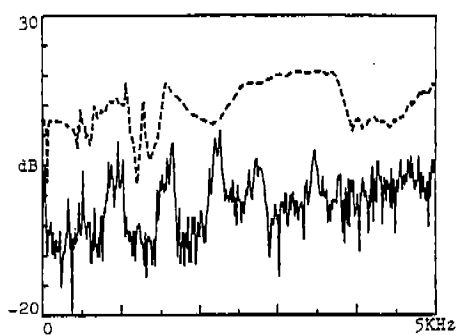


Fig.12 Transfer function of compressor suspension system